International Journal of Automotive Technology, Vol. 7, No. 1, pp. 91–99 (2006)

1229-9138/2006/025-12

MODELING AND PI CONTROL OF DIESEL APU FOR SERIES HYBRID ELECTRIC VEHICLES

B. HE, M. OUYANG* and L. LU

State Key Laboratory of Automotive Safety and Energy, Tsinghua University, Rm. 215, Building 16, Beijing 100084, China

(Received 10 March 2005; Revised 17 August 2005)

ABSTRACT–The diesel Auxiliary Power Unit (APU) for vehicle applications is a complex nonlinear system. For the purpose of this paper presents a dynamic average model of the whole system in an entirely physical way, which accounts for the non-ideal behavior of the diode rectifier, the nonlinear phenomena of generator-rectifier set in an elegant way, and also the dynamics of the dc load and diesel engine. Simulation results show the accuracy of the model. Based on the average model, a simple PI control scheme is proposed for the multivariable system, which includes the steps of model linearization, separate PI controller design with robust tuning rules, stability verification of the overall system by considering it as an uncertain one. Finally it is tested on a detailed switching model and good performances are shown for both set-point following and disturbance rejection.

KEY WORDS : Auxiliary power unit (APU), Series hybrid electric vehicle, Average modeling, Nonlinear system, PI control, Stability

1. INTRODUCTION

As one of the promising solutions to the environmental and energy issues caused by the transportation system, Series Hybrid Electric Vehicle (SHEV) has attracted much attention from the automotive companies and research institutes. Reports (Kelly and Eudy, 2000) show that most of the heavy duty hybrid vehicles are series designs fueled by diesel. SHEV has two power sources, an Auxiliary Power Unit and a battery. With the active control of the APU, the power distribution between them is realized. Hence, it requires that the APU should have good dynamic performances to achieve system-level performance objectives such as vehicle fuel economy and pollution restriction.

The APU system is a nonlinear dynamic integrated system of mechanical, electrical and power electronic devices. To understand the dynamic characteristics of this highly nonlinear system and satisfy the control performance requirements, research on its dynamic modeling and control is a very meaningful but also challenging work.

In the diesel APU, the diesel engine-generator set is connected with a three-phase diode rectifier to drive the dc load. For the rectifier's switching characteristics, continuous modeling for the whole system seems very difficult. With electric circuit simulation tools such as Matlab or PSpice, a detailed switching model of the APU can be obtained to investigate its physical behavior. But it requires a lot of computation time and is not suitable for model-based system analysis and controller design. Average modeling technique was usually used to overcome the limitation, such as the modeling approach for small signal analysis (Sudhoff *et al.*, 1996). For large signal analysis and system-level controller design, an average model was presented in (Jadric *et al.*, 2000), which established a simple relationship between the rectifier's ac input signals and dc output ones. But the model parameters were empirically determined from the switching model simulation and it's only valid in a limited operating range. Based on the average model, PI compensator was designed with the frequency analysis method. (Powell and Pilutti, 1994; Powell *et al.*, 1998) also give an average model, where the generator-rectifier set was simplified to empirical polynomial expressions, and it was only used for system simulation purpose. The PID coupling control strategy of engine speed and generator excitation was discussed.

In this paper we propose a new average model of diesel APU in an entirely physical way. The average model of three-phase diode rectifier considers the non-ideal and dynamic operation of diode rectifier. An average torque production model of diesel engine is built, while the model of synchronous generator uses a classical

*Corresponding author. e-mail: ouymg@tsinghua.edu.cn

one. The whole system model is achieved through the coupling of subsystem models in an elegant way.

Based on the developed average model, a multivariable simplified PI controller is designed for diesel APU. From the system response analysis, the diesel APU can be considered as a two-time-scale system. PI controller with a robust tuning method is designed separately for the speed and dc voltage control. Finally the stability of the overall system is verified by considering the nonlinear system as an uncertain one.

The paper is organized as follows. In Section 2 the configuration and control system of diesel APU is introduced. The average model is described and verified in Section 3. The controller design and its simulation results on the detailed switching model are discussed in Section 4. Finally a conclusion is given in Section 5.

2. DIESEL APU SYSTEM DESCRIPTION

As shown in Figure 1, the diesel APU investigated consists of diesel engine, synchronous generator and three-phase diode rectifier. The dc load of the APU system considered here is a varying resistor parallel with a large dc-link capacitor.

From the structure of diesel APU, we can see that it's a multiple-input multiple-output (MIMO) system. The APU controller regulates the engine speed and dc output voltage through the virtual pedal control of diesel engine and excitation control of generator. For the vehicle applications, the design goals of the diesel APU controller are given as follows:

(1) Engine speed set-point following to ensure the engine operates in its optimized region of high fuel economy and low emissions;
(2) Dc output voltage set-point following to satisfy the varying power needs of loads;
(3) Robust stability of the overall system.

3. AVERAGE MODELING

In such a complex nonlinear system as shown in Figure 1, in order to design properly the control-loops, a detailed time-continuous model of the system is needed. Since the system is comprised of different components, the modeling approach first modeled the subsystems individually,

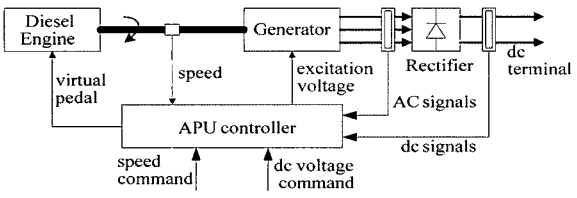

Figure 1. Schematic representation of the diesel APU.

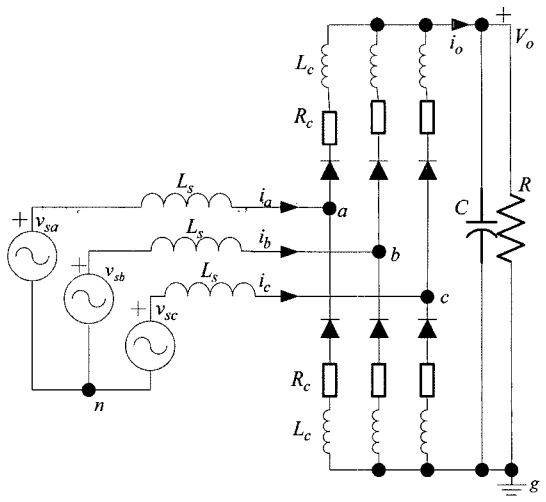

Figure 2. Three-phase diode rectifier circuit.

and then the overall system model is obtained by interconnecting the subsystem models.

3.1. Three-Phase Diode Rectifier Model

The three-phase diode rectifier supplied from an inductive ac source is shown in Figure 2. Three-phase balanced sinusoidal voltages v_{sa}, v_{sb} and v_{sc} with magnitude V_s and angular frequency w are in series with line inductances L_s. An analytical analysis is given in (Caliskan *et al.*, 2003), assuming dc constant voltage V_o and ideal operation of the diodes in the rectifier. Here we will consider a resistor load R parallel with a capacitor C, and non-ideal operation of the diodes with the internal inductance L_c, resistance R_c, and forward on-voltage V_d.

Assuming that source currentsi_a, i_b and i_c vary continuously, the line-to-ground v_{ag}, v_{bg}, v_{cg} and neutral-to-ground voltage v_{ng} are given by

$$v_{ag} = \frac{Vo}{2}+\left(\frac{Vo}{2}+V_d\right)\mathrm{sgn}(i_a)+L_c\frac{di_a}{dt}+R_c i_a \tag{1}$$

$$v_{bg} = \frac{Vo}{2}+\left(\frac{Vo}{2}+V_d\right)\mathrm{sgn}(i_b)+L_c\frac{di_b}{dt}+R_c i_b \tag{2}$$

$$v_{cg} = \frac{Vo}{2}+\left(\frac{Vo}{2}+V_d\right)\mathrm{sgn}(i_c)+L_c\frac{di_c}{dt}+R_c i_c \tag{3}$$

$$v_{ng} = \frac{Vo}{2}+\frac{1}{3}\left(\frac{Vo}{2}+V_d\right)(\mathrm{sgn}(i_a)+\mathrm{sgn}(i_b)+\mathrm{sgn}(i_c)) +\frac{1}{3}L_c\left(\frac{di_a}{dt}+\frac{di_b}{dt}+\frac{di_c}{dt}\right)+\frac{1}{3}R_c(i_a+i_b+i_c) \tag{4}$$

We separate the switching terms from (1)–(4), which are represented by v_{ag}', v_{bg}', v_{cg}' and v_{ng}' given by

$$v_{ag}' = \frac{Vo}{2}+\left(\frac{Vo}{2}+V_d\right)\mathrm{sgn}(i_a) \tag{5}$$

$$v_{bg}' = \frac{Vo}{2}+\left(\frac{Vo}{2}+V_d\right)\mathrm{sgn}(i_b) \quad (6)$$

$$v_{cg}' = \frac{Vo}{2}+\left(\frac{Vo}{2}+V_d\right)\mathrm{sgn}(i_c) \quad (7)$$

$$v_{ng}' = \frac{Vo}{2}+\frac{1}{3}\left(\frac{Vo}{2}+V_d\right)(\mathrm{sgn}(i_a)+\mathrm{sgn}(i_b)+\mathrm{sgn}(i_c)) \quad (8)$$

From the analysis in (Caliskan, 2003), it's known that the switching parts of the circuit equations in (5)–(8) can be approximated in an average manner as an equivalent resistance defined by $R_e=v_{an}'/i_a$. Now consider it with the non-ideal operation terms in (1)–(4), and we can get an equivalent circuit of the three-phase rectifier shown in Figure 3. The equivalent resistance is written as

$$R_e = \frac{V_{o1}^2 R_c + V_{o1}\sqrt{w^2(L_s+L_c)^2(V_s^2-V_{o1}^2)+R_c^2V_s^2}}{V_s^2-V_{o1}^2} \quad (9)$$

where $V_{o1}=4/(\pi)(V_o/2+V_d)$.

As for the dc terminal part, it is just a simple RC circuit. The relationship between the currents of the rectifier's ac and dc terminals is approximated in an average manner as

$$i_o = (3/\pi)\sqrt{i_d^2+i_q^2} \quad (10)$$

where i_o is the average dc current.

Using Park's transformation, the circuit equations of Figure 3 and dc load can be written in the d-q axes as

$$v_d=L_c\frac{di_d}{dt}-wL_ci_q + R_ci_d + R_ei_d \quad (11)$$

$$v_q=L_c\frac{di_q}{dt}-wL_ci_d + R_ci_q + R_ei_q \quad (12)$$

$$v_{sd}=L_s\frac{di_d}{dt}-wL_si_q + v_d \quad (13)$$

$$v_{sq}=L_s\frac{di_q}{dt}-wL_si_d + v_q \quad (14)$$

$$C\frac{dV_o}{dt}+\frac{V_o}{R}=\frac{3}{\pi}\sqrt{i_d^2+i_q^2} \quad (15)$$

where v_{sd}, v_{sq} are source voltages, v_d, v_q are rectifier ac input voltages, i_d, i_q are rectifier ac input currents.

3.2. Synchronous Generator Model

Neglecting the damping windings, a simplified model of synchronous generator is given by (Krause, 1987)

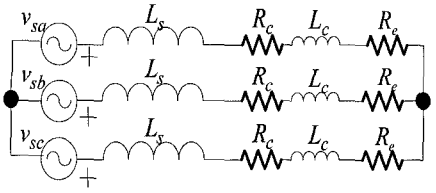

Figure 3. Equivalent circuit of the three-phase rectifier.

$$v_d=-R_si_d-L_d\frac{di_d}{dt}+wL_qi_q+L_m\frac{di_{fd}}{dt} \quad (16)$$

$$v_q=-R_si_q-L_q\frac{di_q}{dt}+wL_di_d+wL_mi_{fd} \quad (17)$$

$$v_{fd}=R_{fd}i_{fd}-L_m\frac{di_d}{dt}+L_{fd}\frac{di_{fd}}{dt} \quad (18)$$

where R_s is stator resistance, R_{fd} is field resistance, L_d is d-axis inductance, L_q is q-axis inductance, L_m is magnetizing inductance, L_{fd} is field inductance, w is angular speed of generator, v_d, v_q are d-axis and q-axis terminal voltages, i_d, i_q are d-axis and q-axis currents, v_{fd} is field voltage, i_{fd} is field current.

For small high speed generators round rotors are often used, where the d-axis and q-axis inductances are equal. We define the inductance L_s as $L_s=L_d=L_q$.

The generator electrical torque is expressed as

$$T_g=1.5pL_mi_{fd}i_q \quad (19)$$

where p is number of pole pairs.

3.3. Diesel Engine Model

For diesel engine, air fuel control and speed control can be separated from each other (Fredriksson and Egardt, 2003). For the engine speed control design, we can only concern the average torque production submodel.

Average indicated torque of diesel engine is given by (Kao *et al.*, 1995)

$$T_m=\eta_{ind}Q_{LHV}m_f \quad (20)$$

where η_{ind} is the engine indicated efficiency, Q_{LHV} is fuel lower heating value, m_f is the mass of fuel injected into the cylinder which is a function of input pedal α and engine speed w_e shown as $m_f(\alpha, w_e)$.

The engine rotational dynamics is given by

$$T_m(t-\tau)-T_g-Dw_e = J\frac{dw_e}{dt} \quad (21)$$

where J is the equivalent rotational inertia of engine-generator set, D is the damping coefficient of engine-generator set, τ is the engine torque delay for the fueling and combustion process delay. The delay τ can be expressed as a function of engine speed

$$\tau = k_1+\frac{k_2}{w_e} \quad (22)$$

where k_1, k_2 are constants (Song and Grigoriadis, 2003).

3.4. Overall System Modeling

Diesel engine and generator are coupled through the mechanical axis. The relationship between engine speed and generator angular speed is given by

$$w_e = \frac{w}{p} \tag{23}$$

Substituting (19), (20), (22), (23) into (21), we obtain

$$\eta_{ind} Q_{LHV} m_f (t-\tau) - 1.5 L_m i_{fd} i_q - \frac{D}{p} w = \frac{J}{p}\frac{dw}{dt} \tag{24}$$

The coupling of generator and three-phase diode rectifier is achieved by considering the diesel engine-generator set as an ac source. We define the ac source as

$$v_{sd} = L_m \frac{di_{fd}}{dt} \tag{25}$$

$$v_{sq} = L_m w i_{fd} \tag{26}$$

As can be seen from (16), (17), the diesel engine-generator set can be interpreted as a source voltage v_{sd}, v_{sq} in series with inductance L_s and resistance R_s. Then, the coupling model is obtained by replacing ac source equations (13), (14) by (16), (17). From (25), (26), we can see that the ac source is controllable with the dynamics of generator excitation current in (18) and engine speed in (24).

With the stator resistance R_s added in (9), the rectifier equivalent resistance for diesel APU is given by

$$R_e = \frac{V_{o1}^2 R_k + V_{o1}\sqrt{(w^2(L_s+L_c)^2(V_s^2 - V_{o1}^2) + R_k^2 V_s^2)}}{V_s^2 - V_{o1}^2} \tag{27}$$

where $R_k = R_s + R_c$.

The average model developed above is an entirely physical one without any fitting parameters. The model parameters are given in Table 1.

Table 1. APU model Parameters.

J	0.3 kg·m^2	D	0.05 N·m·s
k_1	0.0029996	k_2	29.166
R_c	0.001 Ω	L_c	0.675 mH
R_s	0.26 Ω	L_s	14.84 mH
R_{fd}	0.13 Ω	L_{fd}	15.8 mH
L_m	13.7 mH	V_d	1 V
p	1	C	5 mF

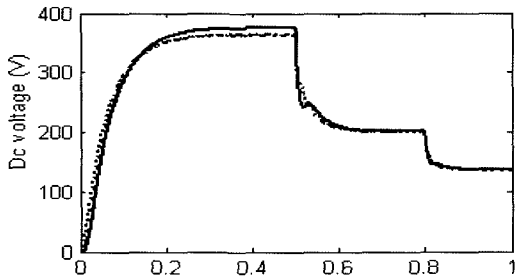

Figure 4. Step response of dc voltage under load change, showing switching model (dotted) and average model (solid).

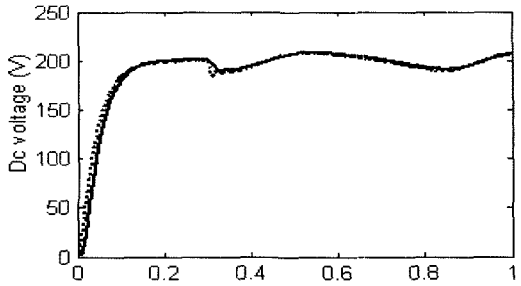

Figure 5. Dc voltage response under speed change, showing switching model (dotted) and average model (solid).

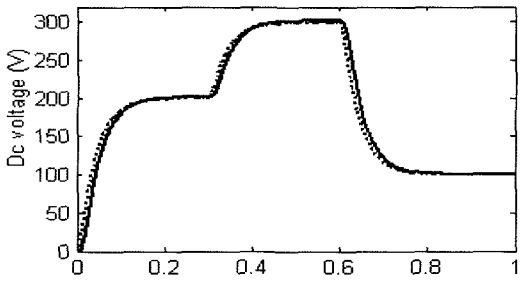

Figure 6. Step response of dc voltage under excitation voltage change, showing switching model (dotted) and average model (solid).

3.5. Model Verification

In order to validate the average model of diesel APU, it is compared with a detailed switching model, which was developed with the SimPowerSystems Toolbox of Matlab. The comparison of simulation results is given respectively in Figure 4, Figure 5 and Figure 6.

In Figure 4, we set $w = 2\pi 50 s^{-1}$, $v_{fd} = 16$ *V*. The initial value of dc load is $R = 3.6$ Ω. Step change occurs at time 0.5s, wher $R = 1.8$ Ω, and at time 0.8s, where $R = 1.2$ Ω.

In Figure 5, we set $R = 1.8$ Ω, $v_{fd} = 16$ *V*. The initial value of engine speed is $w = 2\pi 50$ s^{-1}. Sinusoidal change occurs at time 0.3s, where $w = 2\pi(50+10 \sin 4\pi t)$.

In Figure 6, we set $R = 1.8$ Ω, $w = 2\pi 50 s^{-1}$. The initial value of excitation voltage is $v_{fd} = 16$ *V*. Step change occurs at time 0.3s, where $v_{fd} = 24$ *V*, and at time 0.6s, $v_{fd} = 8$ *V*.

The simulation results all show an excellent matching between the average model and the switching one for both steady state and dynamic behaviors.

4. PI CONTROLLER DESIGN

The mathematical model of the diesel APU above is a

highly nonlinear differential-algebraic system, which to some extent causes the difficulty of direct application of existing nonlinear controller design methods. A simple PID controller was applied to differential-algebraic systems in (Rao *et al.*, 2003), which got the same performance as nonlinear methods. As the first step to real-time control development, we propose a simplified model-based PI control scheme for the diesel APU.

4.1. Continuous Linearized System Model

The engine model developed above has a delay unit. For the continuous model development, the first-order Pade approximation is used

$$e^{-s\tau} \approx \frac{1}{1+\tau s} \tag{28}$$

Then from (24), a second order engine model is derived as

$$\tau \frac{dm_{f1}}{dt} + m_{f1} = m_f(\alpha, w) \tag{29}$$

$$\eta_{ind} Q_{LHV} m_{f1} - 1.5pL_m i_{fd} i_q - \frac{D}{p} w = \frac{J}{p}\frac{dw}{dt} \tag{30}$$

where the new state variable m_{f1} is introduced to consider the delay.

The dynamic model of diesel APU can now be written in a state-space representation. Also, this nonlinear model can be linearized using Taylor's Series expansion at a certain operating condition, which is denoted by a subscript 0

$$E\frac{dx}{dt} = Ax + Bu$$

$$y = Cx \tag{31}$$

with state vector $x = [m_{f1}\ w\ i_{fd}\ i_d\ i_q\ V_0]^T$, input $u = [\alpha\ v_{fd}]^T$, and output $y = [w\ V_0]^T$. The exact form of Jacobian matrices E, A, B and C is shown below

$$E = \begin{bmatrix} \tau_{w0} & 0 & 0 & 0 & 0 & 0 \\ 0 & 0 & -L_m & L_s + L_c & 0 & 0 \\ 0 & 0 & 0 & 0 & L_s + L_c & 0 \\ 0 & 0 & 0 & 0 & 0 & C \\ 0 & J/p & 0 & 0 & 0 & 0 \\ 0 & 0 & L_{fd} & -L_m & 0 & 0 \end{bmatrix} \tag{32}$$

$$A = \begin{bmatrix} -1 & \frac{1}{p}\frac{\partial m_f}{\partial w_0} & 0 & 0 & 0 & 0 \\ 0 & a_{22} & a_{23} & a_{24} & a_{25} & a_{26} \\ 0 & a_{32} & a_{33} & a_{34} & a_{35} & a_{36} \\ 0 & 0 & 0 & a_{44} & a_{45} & -1/R \\ \eta_{ind} Q_{LHV} & -D/p & 0 & 0 & a_{55} & 0 \\ 0 & 0 & -R_{fd} & 0 & 0 & 0 \end{bmatrix} \tag{33}$$

$$\delta = 1/\sqrt{(L_m w_0 i_{fd0})^2 - V_{o10}^2}$$

$$\gamma = (3/\pi)/\sqrt{i_{d0}^2 + i_{q0}^2}$$

$$a_{22} = (L_s + L_c) i_{q0} - (L_s + L_c)(i_{d0} V_{o10}\delta - L_m^2 i_{d0} i_{fd0}^2 w_0^2 V_{o10}\delta^3)$$

$$a_{32} = -(L_s + L_c) i_{d0} + (L_s + L_c)(i_{q0} V_{o10}\delta - L_m^2 i_{q0} i_{fd0}^2 w_0^2 V_{o10}\delta^3)$$

$$a_{23} = (L_s + L_c) L_m^2 i_{d0} i_{fd0} w_0^3 V_{o10}\delta^3$$

$$a_{33} = L_m w_0 (L_s + L_c) L_m^2 i_{q0} i_{fd0} w_0^3 V_{o10}\delta^3$$

$$a_{53} = -1.5pL_m i_{q0}$$

$$a_{24} = a_{35} = -[R_s + R_c + (L_s + L_c) w_0 V_{o10}\delta]$$

$$a_{34} = -(L_s + L_c) w_0$$

$$a_{44} = i_{d0}\gamma$$

$$a_{25} = (L_s + L_c) w_0$$

$$a_{45} = i_{q0}\gamma$$

$$a_{55} = -1.5pL_m i_{fd0}$$

$$a_{26} = -(2/\pi)(L_s + L_c)(w_0 i_{d0}\delta + V_{o10}^2 w_0 i_{d0}\delta^3)$$

$$a_{36} = -(2/\pi)(L_s + L_c)(w_0 i_{q0}\delta + V_{o10}^2 w_0 i_{q0}\delta^3)$$

$$B = \begin{bmatrix} \frac{\partial m_f}{\partial \alpha_0} & 0 & 0 & 0 & 0 & 0 \\ 0 & 0 & 0 & 0 & 0 & 1 \end{bmatrix}^T \tag{34}$$

$$C = \begin{bmatrix} 0 & 1 & 0 & 0 & 0 & 0 \\ 0 & 0 & 0 & 0 & 0 & 1 \end{bmatrix} \tag{35}$$

Using the Control System Toolbox of Matlab, the transfer matrix of the above linearized system is easily obtained as the form

$$\begin{bmatrix} w \\ V_0 \end{bmatrix} = \begin{bmatrix} H_{11} & H_{12} \\ H_{21} & H_{22} \end{bmatrix} \begin{bmatrix} \alpha \\ v_{fd} \end{bmatrix} \tag{36}$$

4.2. Simplified PI Controller Design

The step response of the system (36) around the nominal operating point is shown in Figure 7. It can be seen that the response of diagonal term H_{22} is much faster than that of H_{11}, which results from that the time constants of electrical variables are much faster that mechanical variables. Thus in dealing with electrical dynamics the speed of engine appears to be constant, while dealing with mechanical dynamics electrical transients appear to settle instantaneously. Besides, as diesel engine interacts with generator-rectifier sets only through the mechanical axis, Figure 7 also shows much weaker coupling for the off-diagonal terms H_{12} and H_{21} than the diagonal ones. Hence, for simplified design purpose, the 2×2 MIMO

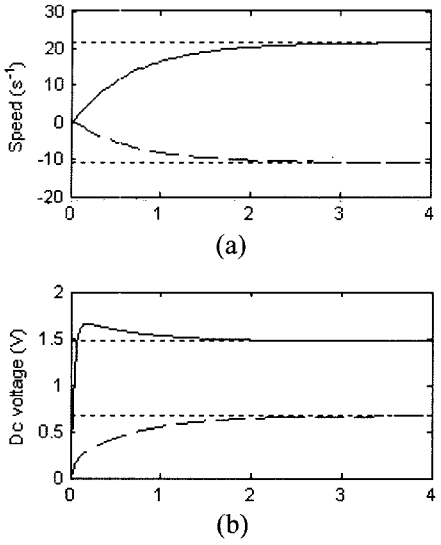

Figure 7. Step response of the diesel APU at the nominal operating point, v_{fd0}=16 V, $R_0 = 3.6\ \Omega$, $w_0 = 2\pi 50 s^{-1}$. (a) Speed response of H_{11} (solid), H_{12} (dotted), (b) Dc output voltage response of H_{22} (solid), H_{21} (dotted).

system can be decomposed into two independent SISO systems neglecting the off-diagonal pairs. But what must be mentioned is that, in fact the two subsystems are still dependent upon each other and finally it must be verified that the two separate control loops will stabilize the overall system in the face of cross-coupling between the loops.

Any standard control design technique can now be applied to the two nominal subsystems. In this paper, the most common PI design method was applied. For controller tuning, Ziegler-Nichols method is a typical tuning method. A new tuning method is proposed in (Hagglund and Astrom, 2002), which is based on the approximate results of robust loop-shaping method that maximize integral gain subject to a constraint on the maximum sensitivity. The tuning rules are given by

$$K = \begin{cases} \dfrac{0.35}{K_v L} - \dfrac{0.6}{K_p}, & \text{for } L < \dfrac{T}{6} \\ \dfrac{0.25T}{K_p L}, & \text{for } \dfrac{T}{6} < L < T \\ \dfrac{0.1T}{K_p L} + \dfrac{0.15}{K_p}, & \text{for } T < L \end{cases} \tag{37}$$

$$T_i = \begin{cases} 7L, & \text{for } L < 0.11T \\ 0.8T, & \text{for } 0.11T < L < T \\ 0.3L + 0.5T, & \text{for } T < L \end{cases} \tag{38}$$

where K_p is static gain, K_v is velocity gain, L is time delay, T is time constant, K and T_i are PI controller parameters.

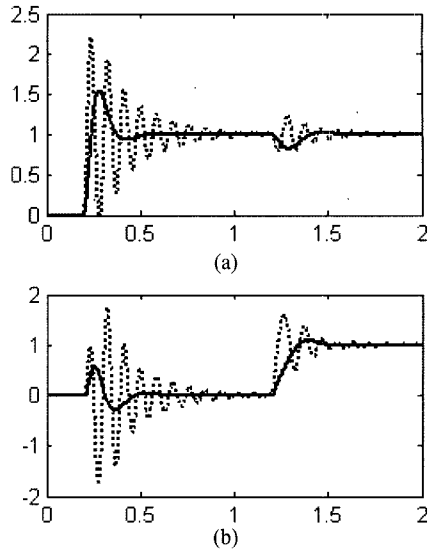

Figure 8. Closed-loop response of the nominal system, for a unit step change of speed command occuring at time 0.2s, and that of dc voltage command occuring at time 1.2s. (a) Speed response, (b) Dc output voltage response. Controller tuned with Ziegler-Nichols method (dotted), with the method in (Hagglund and Astrom, 2002) (solid).

The two tuning methods are both used for the two nominal subsystems. Figure 8 shows the closed-loop response of the nominal system to a set-point change. As can be seen, Ziegler-Nichols method gives highly oscillatory response while the other gives very reasonable response. Besides, what's more important is that, (37) and (38) shows very robust stability performance, which can be seen later in the stability analysis. While with the Ziegler-Nichols method, when diesel APU operates a little far off the nominal conditions, it becomes unstable. Hence we use the tuning rules given by and (38).

The excitation voltage and pedal position have practical limits, $0 \le v_{fd} \le 24V$ $0 \le \alpha \le 100\%$. To overcome the integral wind-up problem in a PI controller caused by the actuator's saturation, a simple anti-windup strategy is used in the form of conditional integration, in which the integrator is stopped when the controller output is saturated and the polarity of the control error is such as to drive the integrator toward the saturated limit.

4.3. Stability Analysis

The PI control scheme proposed above is based on the linearized nominal model. For the nonlinear diesel APU, as the engine speed, excitation voltage or load varies, it will go away from the nominal operating point. On the other hand, the coupling of the two control loops still exists. Hence, the system stability has to be considered.

Now consider the system as a whole, which is shown

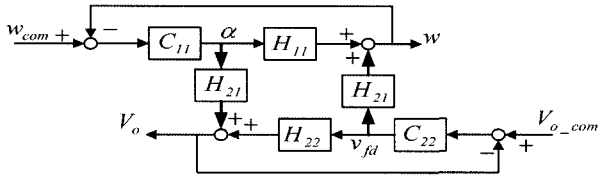

Figure 9. Block diagram for the diesel APU and its control system. C_{11} and C_{22} are PI controllers, w_{com} is the speed command, V_{O_com} is the dc voltage command.

in Figure 9. As the approach in (Senesky *et al.*, 2004), the stability of the system is examined by breaking the loops and finding the open-loop transfer function G

$$G = H_{12}H_{21}\frac{C_{11}}{1+C_{11}H_{11}}\frac{C_{22}}{1+C_{22}H_{22}} \tag{39}$$

The nonlinear function is simply described as uncertainty model set

$$\Pi = \left\{\begin{matrix} P(s)(1+W(s)\Delta(s)) \\ \|\Delta(s)\|_\infty < 1 \end{matrix}\right\} \tag{40}$$

where $P(s)$ is the nominal model, $\Delta(s)$ is the uncertainty, $W(s)$ is a weight function. Using the small gain theorem (Zhou, 1999), the close-loop system is stable if

$$\left\|\frac{W(s)P(s)}{1+P(s)}\right\|_\infty < 1 \tag{41}$$

Robust stability of the diesel APU was verified with the PI controller proposed above in the operating range given below

$$2\pi 30s^{-1} \le w \le 2\pi 60s^{-1},\ 4 \le v_{fd} \le 24V,$$
$$1.2\Omega \le R \le 7.2\Omega \tag{42}$$

4.4. Simulation Results

The above control scheme was developed based on a simplified average model of the system. For its verification, it was tested on the detailed switching model shown in Figure 10.

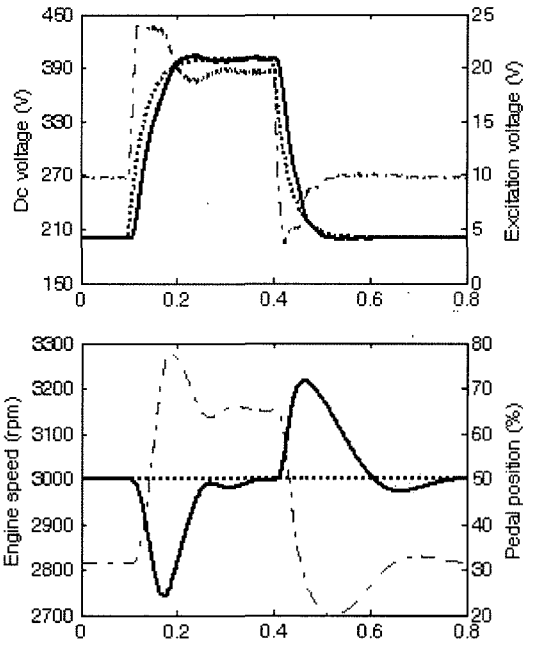

Figure 11. Closed-loop responses of the dc voltage and engine speed, for a set-point change of voltage command (dotted in the upper figure), and constant speed command (dotted in the lower figure). The two control inputs are shown in dash-dotted.

Figure 11 and Figure 12 show system closed-loop responses for set-point commands of dc output voltage and engine speed respectively, which are step change signals that passed through a low pass filter to ensure smooth operation of the diesel APU. The overshoot and settling time characteristics of both dc voltage and speed is satisfactory under the large changes of commands. From the figures, we can also see the coupling phenomena between the engine speed and dc output voltage control loops, showing that the speed oscillation caused by the dc voltage set-point change in Figure 11 is much

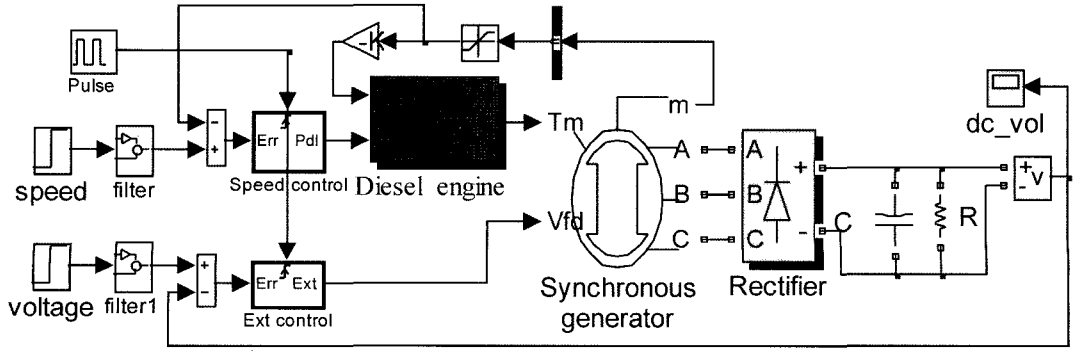

Figure 10. Simulink switching model of the diesel APU.

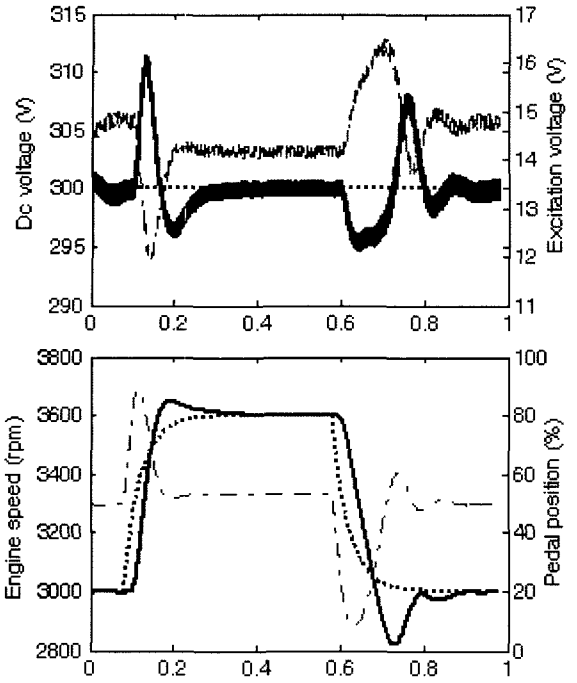

Figure 12. Closed-loop responses of the dc voltage and engine speed, for a set-point change of speed command (dotted in the upper figure), and constant voltage command (dotted in the lower figure). The two control inputs are shown in dash-dotted.

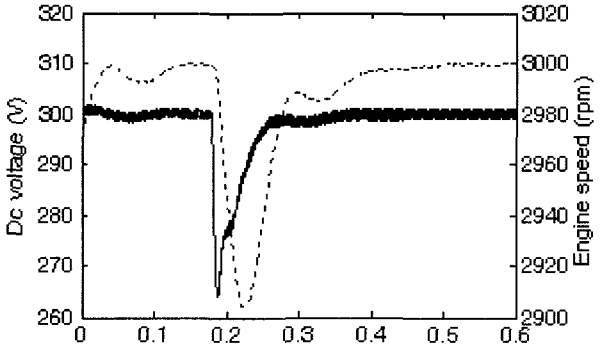

Figure 13. Closed-loop responses of the dc voltage and engine speed for a load step from 3.6 ohm to 2.4 ohm, showing dc voltage (solid), engine speed (dotted).

higher than the contrary in Figure 12 which can be explained by the analysis above. Figure 13 shows the system response under the step load disturbance. The fluctuation of engine speed and dc output voltage is very small and they quickly come back to the equilibrium point. The simulation results of set-point following and load rejection capabilities both show that the PI controllers developed above give very satisfactory performance while ensure system stability.

5. CONCLUSION

A systematic average model of diesel APU has been developed, which preserved all the relevant dynamics of the system for large signal analysis and control design, while accounting for the nonlinear phenomena of rectifiers. The diesel engine and generator-rectifier sets are considered as a whole, so we can investigate the system characteristics and interactions between the subsystems. What's more, it provides the possibility of robust multivariable controller design for the system. The model is entirely a physical one, which is very suitable for large signal analysis, while it has the differential-algebraic characteristics that increase the difficulty of controller design.

For the controller design, the nonlinear average model is simplified to a continuous linear time invariant one with uncertainty. From the system response analysis, we can see that it is a multi-time-scale one, and separate controllers can be designed with the two SISO subsystems. The stability of the overall system is ensured with a robust stability method for the uncertain system. Simulation results show the model's accurateness and the reasonable performances of the controller.

The model developed in this paper is a highly nonlinear one that can be considered as a linear parameter varying system, which suggests that some robust controller design methods such as gain-scheduling may be applied.

As the next step to further investigation for vehicle applications, the diesel APU will be considered under dynamic loads of the battery and induction motor instead of filtered resistor loads in this paper.

REFERENCES

Caliskan, V., Perreault, D. J., Jahns, T. M. and Kassakian, J. G. (2003). Analysis of three-phase rectifiers with constant-voltage loads. *IEEE Trans. Circuits and Systems I: Fundamental Theory and Applications* **50**, **9**, 1220–1225.

Fredriksson, J. and Egardt, B. (2003). Backstepping control with integral action applied to air-to-fuel ratio control for a turbocharged diesel engine. *SAE 2002 Trans. J. Engines*, 506–511.

Hagglund, T. and Astrom, K. J. (2002). Revisiting the zeigler-nichols tuning rules for PI control. *Asian J. Control* **4**, **4**, 364–380.

Jadric, I., Borojevic, D. and Jadric, M. (2000). Modeling and control of a synchronous generator with an active DC Load. *IEEE Trans. Power Electronics* **15**, **2**, 303–311.

Kao, M. H. and Moskwa, J. J. (1995). Turbocharged diesel engine modeling for nonlinear engine control

and state estimation. *ASME J. Dynamic Systems, Measurement, and Control*, **117**, 20–30.

Kelly, K. and Eudy, L. (2000). Field operations program – overview of advanced technology transportation: CY2000. Document NREL/MP-540-27962.

Krause, P. C. (1987). *Analysis of Electric Machinery.* McGraw-Hill. New York.

Powell, B. K., Bailey, K. E. and Cikanek, S. R. (1998). Dynamic modeling and control of hybrid electric vehicle powertrain systems. *IEEE Control Systems Magazine* **18, 5**, 17–33.

Powell, B. K. and Pilutti, T. E. (1994). A range extender hybrid electric vehicle dynamic model. *IEEE 33rd Conf. Decision and Control,* 2736–2741. Lake Bunena Vista, FL.

Rao, N. M., Vora, P. and Moudgalya, K. M. (2003). PID control of DAE systems. *I&EC Research* **1, 42**, 4599–4610.

Senesky, M. K., Tsao, P. and Sanders, S. R. (2004). Simplified modelling and control of a synchronous machine with variable-speed six-step drive. *IEEE APEC Conf.,* **3**, 1803–1809.

Song, Q. and Grigoriadis, K. M. (2003). Diesel engine speed regulation using linear parameter varying control. 2003 American Control Conf., **1**, 779–784.

Sudhoff, S. D., Corzine, K. A., Hegner, H. J. and Delisle, D. E. (1996). Transient and dynamic average-value modeling of synchronous machine fed load commutated converters. IEEE Trans. Energy Conversion **11, 3**, 508–514.

Zhou, K. M. (1999). *Essentials of Robust Control*, 137–145. Prentice Hall, NJ.